High Q X-Band Distributed Bragg Resonator Utilising an Aperiodic Alumina Plate Arrangement

Simon Bale and Jeremy Everard
Department of Electronics
University of York
York, UK
sjb508@ohm.york.ac.uk

***Abstract*—This paper describes an X-Band distributed Bragg resonator which utilizes an aperiodic arrangement of non λ/4 low loss alumina plates mounted in a cylindrical waveguide. An ABCD parameter waveguide model was developed to simulate the cavity. The dielectric plates and air waveguide dimensions were optimized to achieve maximum quality factor by redistributing the energy loss within the cavity. An unloaded quality factor (Q_0) of 196,000 was demonstrated at 9.93 GHz.**

I. INTRODUCTION

The distributed Bragg resonator can offer a substantial increase in quality factor when compared to traditional microwave resonator structures such as the dielectric resonator or empty metal cavity resonator. It is a structure formed by replacing the end and/or side walls of an empty metal cavity with alternating layers of air and dielectric material as shown in fig 1.

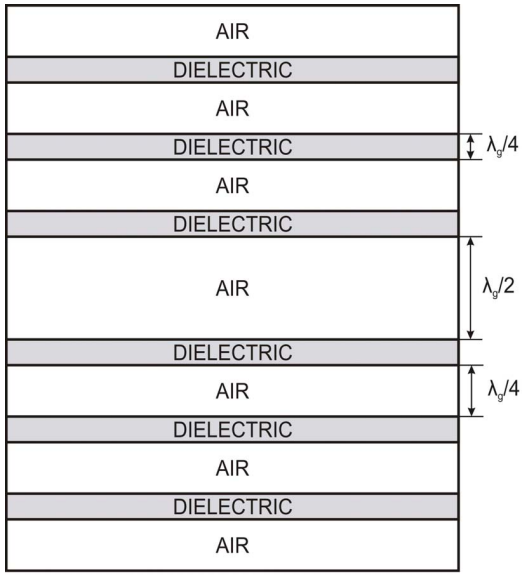

Figure 1. The structure of a periodic Bragg resonator.

The sudden change in dielectric constant at each air dielectric interface causes a partial reflection of the incident electromagnetic wave. If several air-dielectric layers are combined then more of the energy is reflected back into the central air region of the cavity and kept away from the lossy metal end walls. Two distinct classes of distributed Bragg resonator can be identified in the literature and these are the periodic reflector and the aperiodic reflector. In a periodic reflector each of the dielectric plates and air sections are exactly one quarter of the guide wavelength ($\lambda_g/4$) in thickness in order to maximize their reflectivity. Maggiore, Clogston, Spalek, Sailor and Mueller[1] demonstrated a distributed Bragg Sapphire resonator with stated Qs of 5.31×10^5 at 18.99 GHz. Flory and Taber[2] demonstrate experimental results for 9.0 GHz and 13.2 GHz Sapphire resonators consisting of interpenetrating concentric rings and plates with quality factors of 650,000 and 450,000 respectively. In a recent paper Breeze, Krupka and Alford[3] state that the majority of the losses in a periodic Bragg reflector occur in the first quarter wave layer and that by re-distributing the energy into the lower loss air regions, an increase in quality factor can be achieved. They demonstrate (through simulation) that by utilizing an aperiodic arrangement of dielectric plates with thicknesses which asymptotically approach $\lambda_g/4$ as the cavity end walls are reached, a spherical Bragg resonator can be designed with a quality factor in excess 10^7 at 10 GHz. Floch, Tobar and Krupka[4] also demonstrate the development of a simple non-Maxwellian model that allows the design of Bragg resonators with dielectric reflectors of an arbitrary thickness.

In this work we present the design, simulation and measurement results for an X-Band cylindrical distributed Bragg resonator which utilizes an aperiodic arrangement of non λ/4 low loss alumina plates. An ABCD parameter waveguide model has been developed in order to ascertain the potential quality factor that can be achieved from periodic and aperiodic Bragg reflector resonators.

II. RESONATOR MODELLING AND DESIGN

The model described in the following sections represents a cylindrical resonator structure, although the equations could

easily be modified to represent a square or spherical structure. A cylindrical structure was chosen because it offers a simple mechanical construction. The cavity has been designed to operate using the TE_{011} mode at 10 GHz. This is the mode typically chosen for high Q cavities as it exhibits a low inherent loss[5]. It is possible to obtain an increase in Q by designing the cavity to operate using a higher order mode, such as TE_{012}, but this has the disadvantage of increasing the cavity volume.

In our model each air and dielectric section of the Bragg structure is considered to be a separate waveguide which we represent using a two-port network. These two port networks are then cascaded to form the complete Bragg resonator. The ABCD parameter set is used to describe the two port networks because the series cascade connection of these networks reduces to a simple matrix multiplication. Fig. 2 illustrates the cascade connection of an air and dielectric section and the resulting matrix equation.

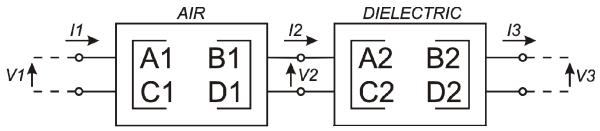

$$\begin{bmatrix} V_1 \\ I_1 \end{bmatrix} = \begin{bmatrix} A_1 & B_1 \\ C_1 & D_1 \end{bmatrix} \begin{bmatrix} A_2 & B_2 \\ C_2 & D_2 \end{bmatrix} \begin{bmatrix} V_3 \\ I_3 \end{bmatrix}$$

Figure 2. A cascade connection of two 2-Port ABCD matrices.

The ABCD matrix must now be defined for each section of the resonator. The ABCD matrix for a lossy transmission line of length l meters with complex propagation constant γ and characteristic impedance Z_0 is shown in (1).

$$\begin{bmatrix} V_1 \\ I_1 \end{bmatrix} = \begin{bmatrix} \cosh \gamma l & Z_0 \sinh \gamma l \\ \frac{1}{Z_0} \sinh \gamma l & \cosh \gamma l \end{bmatrix} \begin{bmatrix} V_2 \\ I_2 \end{bmatrix} \quad (1)$$

In order to correctly represent each section of the resonator using this equation it is necessary to calculate the complex propagation constant and wave impedance for each reflector section. These calculations are performed assuming the wave is travelling in a cylindrical wave guide. The complex propagation constant, γ, is defined by (2).

$$\gamma = \alpha + j\beta \quad (2)$$

Where α is the attenuation coefficient measured in units of Npm^{-1} and β is the phase constant. The phase constant for the dielectric and air sections can be calculated from (3).

$$\beta = \sqrt{\omega^2 \mu\varepsilon - \left(\frac{\chi`_{mn}}{a}\right)^2} \quad (3)$$

Where ε is the permittivity of the material filling the guide, ω is the angular frequency and a is the cavity radius. $\chi`_{mn}$ represents the $n^{th}$ zero of the derivative of the Bessel function of the first kind of order $m$. In the case of the $TE_{01}$ mode the value of $\chi`_{mn} \approx 3.8318$.

A. Air Sections

The only loss in the air filled sections of the guide is a result of the conductive side walls. This can be calculated using the perturbation method as described in [6] and the resulting equation is show in (4). This equation represents the attenuation coefficient, in units of Npm^{-1}, for a transverse electric (TE) mode with circumferential mode number m and radial mode number n in a cylindrical waveguide of radius a operating at frequency, f.

$$\left(\alpha_c\right)_{mn}^{TE_Z} = \frac{R_s}{a\eta\sqrt{1-\left(\frac{f_c}{f}\right)^2}}\left[\left(\frac{f_c}{f}\right)^2 + \frac{m^2}{\left(\chi`_{mn}\right)^2 - m^2}\right] \quad (4)$$

Where η, given in (5), is the wave impedance for a plane wave inside an unbounded infinite medium with permittivity, ε and permeability μ.

$$\eta = \sqrt{\frac{\mu}{\varepsilon}} \quad (5)$$

The surface loss resistance of the guide walls is represented by R_s and this is a function of the wall conductivity σ. The value of R_s can be calculated using (6).

$$R_s = \sqrt{\frac{\omega\mu}{2\sigma}} \quad (6)$$

The lower cut of frequency of the guide is give by f_c and its value can be calculated using (7).

$$f_c = \frac{\chi`_{mn}}{2\pi a\sqrt{\mu\varepsilon}} \quad (7)$$

The only remaining term required to describe ABCD matrix for the air filled sections is the guide wave impedance Z_0. This can be calculated for a transverse electric mode using (8).

$$Z_{TE} = \frac{\eta}{\sqrt{1-\left(\frac{f_c}{f}\right)^2}} \quad (8)$$

B. Dielectric Sections

For the lossy dielectric sections we must consider the dielectric loss introduced by the Alumina plates. This can be calculated by considering the total loss in dielectric sections, α_t, as the sum of the sidewall conducting loss, α_c, and the dielectric losses, α_d.

$$\alpha_t = \alpha_c + \alpha_d \tag{9}$$

The attenuation due to the lossy dielectric, α_d, can be calculated directly from the complex propagation constant as shown in [7]. If the loss is small then the phase constant in the dielectric section will remain unchanged. The attenuation due to dielectric loss is given by equation (10).

$$\alpha_d = \frac{\omega^2 \mu\varepsilon \tan\delta}{2\sqrt{\omega^2 \mu\varepsilon - \left(\frac{\chi'_{mn}}{a}\right)^2}} \tag{10}$$

Where *tan δ* is the loss tangent of the dielectric and ε is the relative permittivity of the dielectric.

C. Metal End Walls

The loss in the metal end walls of the cavity can be approximated by considering the complex propagation constant, γ, and intrinsic wave impedance, η, for a plane in a good conductor. As is described in [8], the complex propagation constant inside a good conductor is given by (11).

$$\gamma = j\omega\sqrt{\mu\varepsilon}\sqrt{\frac{\sigma}{j\omega\varepsilon}} \tag{11}$$

This can be rearranged into the form show in (12).

$$\gamma = (1+j)\sqrt{\frac{\omega\mu\sigma}{2}} \tag{12}$$

The intrinsic wave impedance for a plane wave in a general lossy medium is given by (13).

$$\eta = \frac{j\omega\mu}{\gamma} \tag{13}$$

If we now substitute (11) into (13) and re-arrange then we can write (14).

$$\eta = (1+j)\sqrt{\frac{\omega\mu}{2\sigma}} \tag{14}$$

Equation (14) describes the wave impedance inside a good conductor. It can be seen that the real and imaginary parts of (14) can be modeled as an impedance consisting of a series connected resistance and inductance. In terms of ABCD parameters this can be written as (15).

$$\begin{bmatrix} V_1 \\ I_1 \end{bmatrix} = \begin{bmatrix} 1 & 0 \\ 1/\eta & 1 \end{bmatrix} \begin{bmatrix} V_2 \\ I_2 \end{bmatrix} \tag{15}$$

Using the equations (1) to (14) it is now possible to entirely characterize a dielectric, air or metal end wall section of the Bragg resonator in terms of its ABCD parameters. This model offers several advantages when compared to a full field simulation. It is possible to model a Bragg resonator with any number of dielectric and air sections of arbitrary lengths. The computation requirements are minimal and the resonant frequency and quality factor for a given mode can be extracted very rapidly using standard circuit simulation techniques. One disadvantage of the model is that it considers each mode in isolation and therefore to calculate the resonant frequencies of other modes additional simulations are required.

III. Periodic Resonator Simulation

A simulation of a microwave periodic Bragg resonator has been performed using the model described in the previous section. The cavity radius was assumed to be 60 mm and the central section length was calculated to ensure that the TE_{011} resonance would occur at 10 GHz. The lengths of the air and dielectric sections were set to one quarter of the guide wavelength, ($\lambda_g/4$) at the resonant frequency. The parameters used in the simulation are shown in fig. 3.

Parameter	Value
Dielectric Section Length	2.41 mm
Air Section Length	7.87 mm
Central Section Length	15.73 mm
Dielectric Permittivity	9.75
Dielectric Loss Tangent	1×10^{-5}
Cavity Radius	60 mm
Wall Conductivity	6.1×10^{7} Sm^{-1}

Figure 3. Periodic Bragg resonator simulation parameters.

Several simulations were performed using varying numbers of dielectric plates. The results are shown in fig. 4.

Number of Dielectric Plates	Unloaded Quality Factor (Q_0)
2	125,785
4	289,854
6	322,579
8	327,867
10	327,867

Figure 4. The simulated unloaded quality factor for periodic Bragg resonators with varying numbers of dielectric plates.

It can be seen from these results that the unloaded quality factor begins to saturate when more than six plates are used. The quality factor of the periodic Bragg design could be further improved by increasing the cavity radius in order to reduce the wall loss. However, this has the undesirable affect of increasing the number of spurious modes.

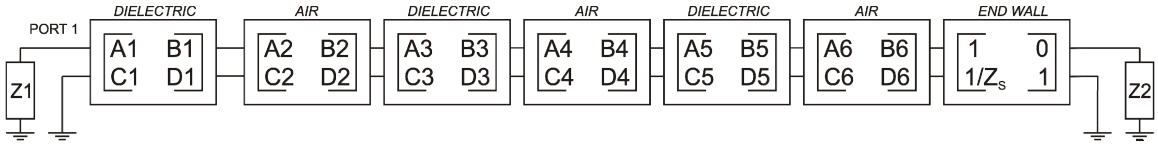

Figure 5. A waveguide ABCD parameter model for one half of a six plate Bragg resonator. The air and dielectric plate thicknesses of this structure are optimised to maximise the magnitude of the input reflection coefficient (S_{11}).

IV. A-Periodic Resonator Simulation

Breeze, Krupka and Alford[3] have demonstrated that a significant improvement in the quality factor of a Bragg resonator can be achieved by utilizing an aperiodic plate arrangement to re-distribute the energy inside the cavity into the lower loss air sections. In order to ascertain the reflector thicknesses required for maximum Q in our resonator a numerical optimization procedure was adopted.

In this new model only one half of the Bragg resonator is considered. The structure to be simulated is illustrated in fig. 5. The value of port impedance, Z_1, was set equal to the wave impedance inside an air section. This ensures that we are representing a wave travelling from the central air region towards a dielectric plate. The value of terminating impedance, Z_2, is less critical due to the small impedance to ground presented by the end wall. However, its value must be large enough to avoid reducing the end wall impedance.

The air and dielectric section thicknesses were initially set to the values used in the periodic design as shown in fig. 3. The reflector section lengths were then optimized until the magnitude of the input reflection coefficient at port one (S_{11}) reached a maximum. When an optimal set of plate thicknesses was found two half resonators were combined and then the central air section was re-introduced. The final stage of the optimization required that length of the central resonant region was adjusted in order to restore the desired resonance to the correct frequency. A simulation of the complete Bragg structure was then be performed. Using this optimization algorithm it has been possible to design a cavity with a simulated unloaded quality factor of 400,000 at 10 GHz.

V. Current Results

Using the model and simulation results described in the previous section a cylindrical Bragg resonator has been constructed which utilizes an aperiodic arrangement of Alumina plates.

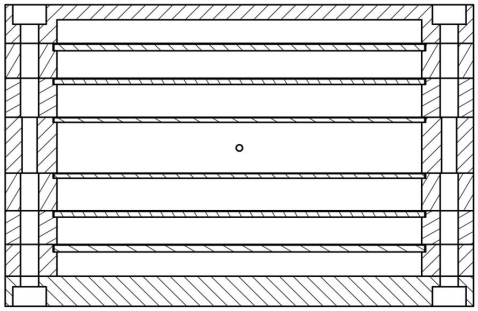

Figure 6. A cross section view of the 6 plate aperiodic Bragg resonator

The resonator has been designed to operate using the TE_{011} low loss mode with a resonant frequency of 10 GHz. A cross sectional view of the cavity is shown in fig 6. This initial design consists of six dielectric plates mounted in an Aluminum shield. Wire loop probes were used to couple energy into the cavity. Fig. 7 shows a photo of the central air filled resonant section and the wire loop coupling probes.

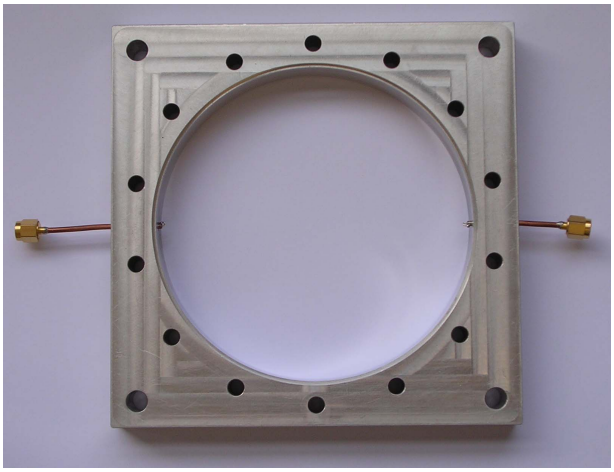

Figure 7. A-periodic Bragg resonator central air filled section.

A plot of the forward transmission coefficient scattering parameter (S_{21}) is show in fig. 8. The wanted resonance can be seen at the centre of this plot. Several spurious modes are also clearly visible.

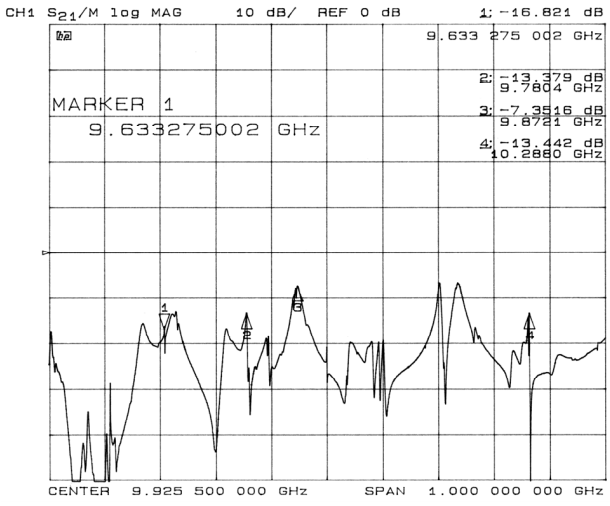

Figure 8. A plot of the forward transmission coefficient (S_{21}) for the 6 plate aperiodic Bragg resonator. A frequency span of 1 GHz is shown.

A narrow band plot of the wanted resonance is show below in fig. 9. It can be seen that the resonator has a centre frequency of 9.94 GHz with a loaded quality factor, Q_L, of 126,810 and an insertion loss, S_{21} of -8.98dB.

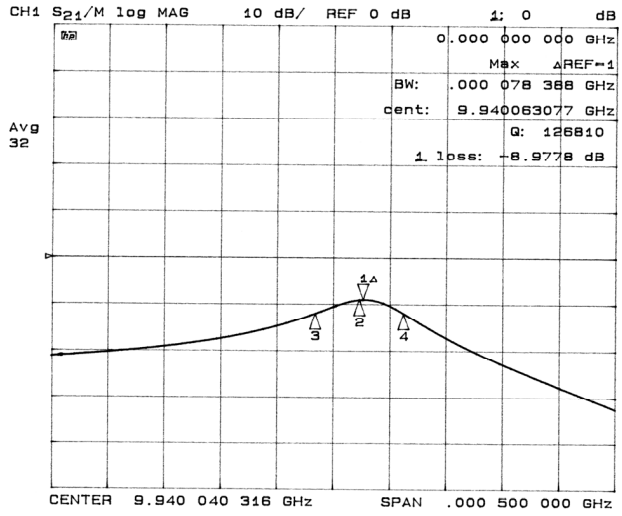

Figure 9. A plot of the forward transmission coefficient (S_{21}) for the 6 plate aperiodic Bragg resonator. A frequency span of 500 kHz is shown.

The unloaded quality factor, Q_0, can be calculated using (16).

$$Q_0 = \frac{Q_L}{(1 - S_{21})} \tag{16}$$

Where Q_L is the loaded quality factor and S_{21} is the insertion loss in linear form. Substituting the values above gives an unloaded quality factor, Q_0, of 196,797.

VI. Conclusions

The resonant frequency of 9.94 GHz is in good agreement with the simulated result of 10 GHz. However, the unloaded quality factor of 196,797 is considerably lower that the simulated value of 400,000. The increased loss in the resonator is thought to be due to an increase in wall losses resulting from the poor conductivity of the resonator shield; an increase in the loss tangent of the alumina plates and the introduction of discontinuities as a result of the structures required to support the dielectric plates.

Acknowledgment

We wish to thank BAE Systems, the Royal Academy of Engineering and the University of York for supporting this work.

References

[1] C.J. Maggiore, A.M. Clogston, G. Spalek, W. Sailor, and F.M. Mueller, "Low-loss microwave cavity using layered dielectric materials," Applied Physics Letters, vol. 64, issue 11, pp. 1451-1453, Mar. 1994.

[2] C.A. Flory, R.C. Taber, "High performance distributed Bragg reflector microwave resonator," IEEE Trans. Ultrasonics, Ferroelectrics and Frequency Control, vol. 44, no. 2, pp. 486-495, Mar. 1997.

[3] J. Breeze, J. Krupka and N.M. Alford. "Enhanced quality factors in aperiodic reflector resonators," Applied Physics Letters, vol. 91, issue 15, Oct. 2007.

[4] J.M. le Floch, M.E. Tobar, D. Cros and J. Krupka "High Q-factor distributed bragg reflector resonators with reflectors of arbitrary thickness," IEEE Trans. Ultrasonics, Ferroelectrics and Frequency Control, vol. 54, no. 12, pp. 2689-2695, Dec. 2007.

[5] D.M. Pozar, "Microwave Engineering," 3rd ed., USA: Wiley, 2005, pp. 284-287.

[6] C.A. Balanis, "Advanced Engineering Electromagnetics," USA: Wiley, pp. 485-488.

[7] D.M. Pozar, "Microwave Engineering," 3rd ed., USA: Wiley, 2005, pp. 97-98.

[8] D.M. Pozar, "Microwave Engineering," 3rd ed., USA: Wiley, 2005, pp. 18-19.